World Academy of Science, Engineering and Technology
International Journal of Electronics and Communication Engineering
Vol:3, No:2, 2009

Lower energy Gait Pattern Generation in 5-Link Biped Robot Using Image Processing

Byounghyun Kim, Youngjoon Han, and Hernsoo Hahn

Abstract**—** The purpose of this study is to find natural gait of biped robot such as human being by analyzing the COG (Center Of Gravity) trajectory of human being's gait. It is discovered that human beings gait naturally maintain the stability and use the minimum energy. This paper intends to find the natural gait pattern of biped robot using the minimum energy as well as maintaining the stability by analyzing the human's gait pattern that is measured from gait image on the sagittal plane and COG trajectory on the frontal plane. It is not possible to apply the torques of human's articulation to those of biped robot's because they have different degrees of freedom. Nonetheless, human and 5-link biped robots are similar in kinematics. For this, we generate gait pattern of the 5-link biped robot by using the GA algorithm of adaptation gait pattern which utilize the human's ZMP (Zero Moment Point) and torque of all articulation that are measured from human's gait pattern. The algorithm proposed creates biped robot's fluent gait pattern as that of human being's and to minimize energy consumption because the gait pattern of the 5-link biped robot model is modeled after consideration about the torque of human's each articulation on the sagittal plane and ZMP trajectory on the frontal plane. This paper demonstrate that the algorithm proposed is superior by evaluating 2 kinds of the 5-link biped robot applied to each gait patterns generated both in the general way using inverse kinematics and in the special way in which by considering visuality and efficiency.

Keywords**—**5-link biped robot, gait pattern, COG (Center Of Gravity), ZMP (Zero Moment Point).

I. INTRODUCTION

THE human has evolved to minimize of energy with natural gait. Human-shaped biped robot can have high efficiency when it follows human's gait pattern. However, it has lots of limitations with movement unlike human. Humanoid robot, therefore, depends on its wheels for safe movement. But the studies about safety of gait of biped robot is an actively area of research.

Magdalena[1] has presented gait pattern by usinf fuzzy system based on standard gait pattern. Huang[2] has generated the pattern by applying trajectory of hip and foot of robot. Endo[3] has done research in order to make optimization of gait through the set of initial values, evolve-operate and decision of GA. The existing studies about biped robot have limitations with natural movements because they focused to make suitable gait pattern of two feet robot's structure.

To make the gait pattern of a robot, Vukobratobic[4] has proposed the Zero Moment Point(ZMP) which can decide the state of dynamical balance. To get the ZMP, Kajita[5] used inverted pendulum model which simplifies man's shape into a joint and a link. Huang [6] has created the trajectory of foot and waist which suit with safe area made by the sole of a foot after it sets the ZMP which fits safety of gait. Arbulu[7] attached the pressure sensor to the bottom of a foot to get man's ZMP. Then it has got ZMP trajectory by getting the entire degree leaning. Most of these focus on two dimension of COG. But Morisawa[8] considered the three dimension.

The study about gait pattern is to analyze natural man's gait by securing safety. Hasegawa[9] defines that robot's natural movement is to minimize the energy. It leads the natural and safe movements used by the class-structural evolution algorithm. This performs the study about natural gait of the biped robot by analyzing man's COG trajectory.

The proposed method generates robot's pattern by analyzing man's from an image on the sagittal plane and frontal plane. It's similar frame and difference structure of degree of freedom between the man and robot. That is the reason why we can't apply the torque from man. To make it, we make the pattern of the 5-link-robot through the suitable GA which uses measured torque and ZMP from man's gait pattern. The proposed algorithm makes the pattern which minimize the energy loss by considering these factors.

This paper organized as follows. Section II explains how to model the gait pattern. Section III describes the analysis of ZMP measured from COG trajectory of human's gait. Section IV analyzes and gets the torque of each joint from an image of human's gait pattern. Section V presents the gait pattern method of the biped robot. Experiments of the gait pattern generations and simulations about the biped robot are shown in Section VI. Section VII describes the conclusions.

II. THE HUMAN AND 5-LINK BIPED ROBOT`S MODELING OF THE GAIT PATTERN

It is difficult for the human's gait pattern to be applied to biped robot model because it has the complicated mechanical structure. Therefore, the human model for the gait analysis needs to be as possible as simple. From this point of view, physiologists show that the most walking dynamics takes place on the sagittal plane[10]. Hence, this paper uses a 5-link biped

Byounghyun Kim is with the Electronics Engineering Department, Soongsil University, 511 Dongjak-Gu, Seoul, KOREA (corresponding author to provide phone: 02-821-2050; fax: 02-826-8937; e-mail: forcera1@naver.com).

Youngjoon Han is with the Electronics Engineering Department, Soongsil University, 511 Dongjak-Gu, Seoul, KOREA (corresponding author to provide phone: 02-820-0699; fax: 02-826-8937; e-mail: young@ssu.ac.kr).

Hernsoo Hahn is with the Electronics Engineering Department, Soongsil University, 511 Dongjak-Gu, Seoul, KOREA (corresponding author to provide phone: 02-820-0709; fax: 02-826-8937; e-mail: hahn@ssu.ac.kr).

robot model to approximate the human's complex mechanical structure in the image sequences.

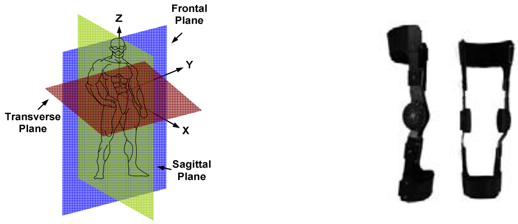

(a) Definition of the plane (b) Restrictive walking device

Fig. 1 Definition of sagittal, frontal and transverse plane, and mechanical parts constraining human walking to sagittal plane

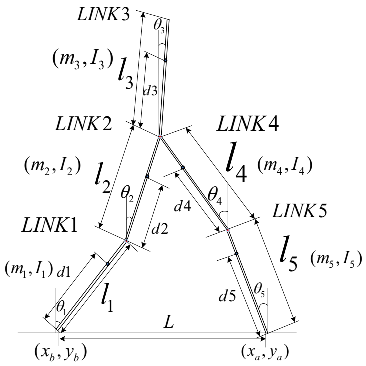

Fig. 2 Values of 5-link biped model

The helpful walking device as shown in Fig. 1(b) is used so that the human's walking movement is limited to sagittal plane. That is, the human's walking pattern is limited to X-Z plane.

The 5-link biped robot is constructed as shown in Fig. 2. The biped robot consists of five links, a torso and two legs. It also has two pelvises at the hip, two knees between the thighs and the shanks, and two ankles at the tips of the two limbs. All of the joints can only rotate on the sagittal plane and have no friction. Feet are not considered in this 5-link biped robot. The 5-link biped robot parameters are represented as follows.

m_i	mass of link i_{th}
l_i	length of link i_{th}
d_i	distance from joint i_{th} to the center of mass of link i_{th}
I_i	moment of inertia of link i_{th} about the axis passing through the center of mass of link i_{th} and perpendicular to the sagittal plane
θ_i	angle of link i_{th} about the vertical
(x_b,y_b)	the coordinate of the supporting point
(x_a,y_a)	the coordinate of the tip of the swing limb
τ_i	torque of joint i_{th}

For measuring these parameters, a subject puts on the restrictive walking device and attaches three markers to his pelvis, knee and ankles as shown in Fig. 3. These parameters of human's joints are measured from sequential images of the human gait on the sagittal plane.

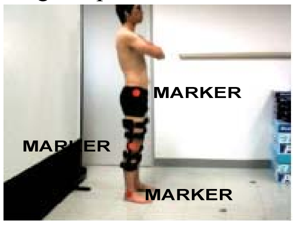

Fig.3 Location of the markers and approximation of model using a 5-link biped model

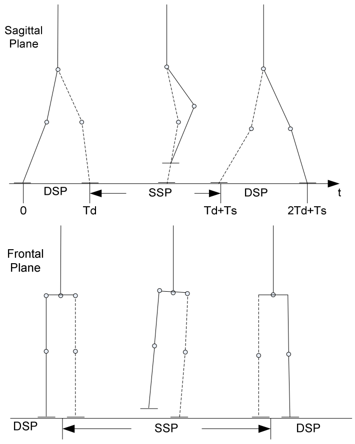

Fig. 4 Gait phases on the sagittal and frontal plane

To associate the 5-link biped robot's gait with the human's gait, torques applied to the human joints are analyzed during walking. The analysis makes it to estimate how much torques are applied to joints of the 5-link biped robot. This paper uses the average length and mass of each human link, and calculates the human's joint torques and 5-link biped robot's ones using dynamic model of Lagrangian equation [11, 12].

The 5-link biped robot's gait is composed periodically of Double Support Phase (DSP) and Single Support Phase (SSP). In Fig.4, T_d and T_s are times of DSP and SSP period respectively.

A. Single Support Phase (SSP)

The SSP is a state that one leg of the biped robot swings and the other leg is in contact with the ground. According to figure 1, The coordinates of the center of mass link i are

$$x_{ci} = \sum_{j=1}^{i-1}(a_j l_j \sin\theta_j) + d_i \sin\theta_i + x_b \quad (1)$$

$$y_{ci} = \sum_{j=1}^{i-1}(a_j l_j \cos\theta_j) + d_i \cos\theta_i + y_b$$

Where (x_{ci}, y_{ci}) is the coordinates of the Center of mass link i, a_i is 0 case of the link3 else 1. Thus, 5-link biped model's the potential energy and the kinetic energy are expressed by Eq. (2), Eq. (3).

$$\begin{aligned} P &= \sum_{i=1}^{5} m_i g y_{ci} \\ &= \sum_{i=1}^{5}[m_i g[\sum_{j=1}^{i-1}(a_j l_j \cos\theta_j) + d_i \cos\theta_i]] \end{aligned} \quad (2)$$

$$\begin{aligned} K &= \sum_{i=1}^{5}[\frac{1}{2} m_i(\dot{x}_{ci}^2 + \dot{y}_{ci}^2) + \frac{1}{2} I_i \dot{\theta}_i^2] \\ &= \sum_{i=1}^{5}[\frac{1}{2}(I_i + m_i d_i^2)\dot{\theta}_i^2] \\ &+ \sum_{i=1}^{5}[\frac{1}{2} m_i[\sum_{j=1}^{i-1}(a_j l_j \dot{\theta}_j \cos\theta_j)]^2] \\ &+ \sum_{i=1}^{5}[\frac{1}{2} m_i[\sum_{j=1}^{i-1}(a_j l_j \dot{\theta}_j \sin\theta_j)]^2] \\ &+ \sum_{i=1}^{5}[m_i d_i \dot{\theta}_i \sum_{j=1}^{i-1}[a_j l_j \dot{\theta}_j \cos(\theta_i - \theta_j)]] \end{aligned} \quad (3)$$

By applying equations (2) and (3) to the Lagrangian formulation, the dynamic model for the 5-link biped model during the SSP can be derived as Eq. (6).

$$L = K - P \quad (4)$$

$$\frac{d}{dt}\frac{\partial L}{\partial \dot{\theta}_i} - \frac{\partial L}{\partial \theta_i} = \tau_i \quad (5)$$

$$D(\theta)\ddot{\theta} + H(\theta,\dot{\theta})\dot{\theta} + G(\theta) = \mathrm{T} \quad (6)$$

Where $D(\theta)$ is the 5x5 positive definite and symmetric inertia matrix, $H(\theta,\dot{\theta})$ is the 5x5 matrix related to centrifugal and coriolis terms, $G(\theta)$ is the 5x1 matrix of gravity terms, $\theta, \dot{\theta}, \ddot{\theta}$ and T are the 5x1 vectors of generalized coordinates, velocities, accelerations and torques.

B. Double Support Phase (DSP)

On the DSP, both of the feet are in contact with the ground. Since the contact position between the two tips of the limbs and the ground are known during DSP, a set of holonomic constraint is given as Eq. (7).

$$\begin{aligned} \Phi(\theta) &= \begin{bmatrix} f_1 \\ f_2 \end{bmatrix} = \begin{bmatrix} x_a - x_b - L \\ y_a - y_b \end{bmatrix} = 0 \\ \Phi(\theta) &= \begin{bmatrix} l_1 \sin\theta_1 + l_2 \sin\theta_2 + l_4 \sin\theta_4 + l_5 \sin\theta_5 - L \\ l_1 \cos\theta_1 + l_2 \cos\theta_2 - l_4 \cos\theta_4 - l_5 \cos\theta_5 \end{bmatrix} \end{aligned} \quad (7)$$

Where L is the distance of the tips of the two limbs. In order to be applied to the dynamic derivation, it is differentiated twice with respect to time as given in Eq. (8).

$$\begin{aligned} J(\theta) &= \frac{\partial\Phi(\theta)}{\partial\theta} \\ \dot{\Phi} &= J(\theta)\dot{\theta} = 0 \\ \ddot{\Phi} &= \dot{J}(\theta)\dot{\theta} + J(\theta)\ddot{\theta} = 0 \end{aligned} \quad (8)$$

Where $J(\theta)$ is the Jacobian matrix. The vector equation of the dynamics on DSP is given Eq. (9).

$$D(\theta)\ddot{\theta} + H(\theta,\dot{\theta})\dot{\theta} + G(\theta) = J^T(\theta)\lambda + \mathrm{T} \quad (9)$$

Where λ is 2x1 vector of Lagrange multipliers.

We need solve the λ from the constraint conditions for the model. The Jacobian matrix is not a square matrix so that the multipliers cannot be calculated directly. So to solve this problem, multypling JD^{-1} to both sides of Eq. (10).

$$J\ddot{\theta} + JD^{-1}h = (JD^{-1}J^T)\lambda + JD^{-1}\mathrm{T} \quad (10)$$

Where $h = H(\theta,\dot{\theta})\dot{\theta} + G(\theta)$, and $JD^{-1}J^T$ is positive definite. Thus it is invertible. So λ can be calculated. $JD^{-1}J^T$ is called pseudo Jacobian matrix, which is powerful in solving the inverse kinematics if the Jacobian is not invertible. The dynamics equations of DSP are finally written as Eq. (11)

$$\begin{aligned} \ddot{\theta} &= D^{-1}((\mathrm{T} - h) + J^T\lambda) \\ \lambda &= -(JD^{-1}J^T)^{-1}(JD^{-1}(\mathrm{T} - h) + J\ddot{\theta}) \end{aligned} \quad (11)$$

III. Analysis of the ZMP of the Human's Gait

The dynamics analysis about the human's gait is described by Human's COG according to Newton's second Law that external force of act on object is same to multiply object's mass with center of mass's acceleration[13]. So when we analyze the COG motion, human's body structure can be represented by a single inverted pendulum which connects the supporting foot and the center of mass of the whole robot as shown Fig. 5.

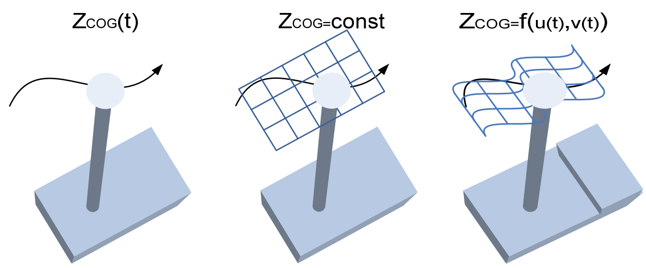

(a) Time Base (b) Constraint plane base (c) Constraint surface base

Fig. 5 COG motion models according to the COG trajectory of inverted pendulum model

Here, time base approach (a) provides a vertical COG motion as a time function. Constraint plane approach (b) shows the vertical velocity of the COG is constant which is derived by analytical solution of the linear inverted pendulum. Constraint surface approach (c) means the COG motion follows desired surface. In this approach, the spatially natural gait pattern is generated on the motion surface which is designed by considering a landing position and a movable space of legs. The ZMP trajectory that is the stable pose of the biped robot is acquired by using the COG trajectory information.

Fig. 6 Markers attached on the center of gravity in the frontal plane

A. Linear Inverted Pendulum

Generally, humanoid robot can be expressed as the COG and the angular momentum around the COG as shown in Fig. 7[8].

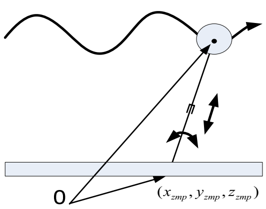

Fig. 7 Inverted pendulum model

Let $x_G = [x_G, y_G, z_G]^T$ be the trajectory of the COG corresponding the ZMP trajectory. Also, let $L_G = [L_{Gx}, L_{Gy}, L_{Gz}]^T$ be the angular momentum of the robot about the COG. When the external force does not act to humanoid robot, the ZMP position can be calculated as,

$$x_{zmp} = \frac{M(x_G(\ddot{z}_G + g) - (z_G - z_{zmp})\ddot{x}_G) - \dot{L}_{Gy}}{M(\ddot{z}_G + g)} \quad (12)$$

$$y_{zmp} = \frac{M(y_G(\ddot{z}_G + g) - (z_G - z_{zmp})\ddot{y}_G) + \dot{L}_{Gx}}{M(\ddot{z}_G + g)} \quad (13)$$

Where, M is a total weight of humanoid robot, g is gravity acceleration. Here, since the influence of angular momentum during walking is small, let us assume the angular momentum can be neglected in the ZMP equations

$$x_{zmp} = x_G - \frac{(z_G - z_{zmp})\ddot{x}_G}{\ddot{z}_G + g} \quad (14)$$

$$y_{zmp} = y_G - \frac{(z_G - z_{zmp})\ddot{y}_G}{\ddot{z}_G + g} \quad (15)$$

Looking at Eq. (14) and Eq. (15), it is observed that two ZMP equations include three translational variables. Therefore, the COG motion can not be specified arbitrarily. Let us express the COG motion as parametric surface.

$$\begin{aligned} x_G &= a(u(t), v(t)) \\ y_G &= b(u(t), v(t)) \\ z_G &= c(u(t), v(t)) \end{aligned} \quad (16)$$

Where, a, b and c are functions which characterize the shape of surface. $u(t)$ and $v(t)$ are parameters which make a time response on the constraint surface. Substituting Eq. (5) into Eq. (12) and Eq. (13), the ZMP position are rewritten as

$$x_{zmp} = a - \frac{(c - z_{zmp})(a_u\ddot{u} + a_v\ddot{v} + a_{uu}\dot{u}^2 + 2a_{uv}\dot{u}\dot{v} + a_{vv}\dot{v}^2)}{c_u\ddot{u} + c_v\ddot{v} + c_{uu}\dot{u}^2 + 2c_{uv}\dot{u}\dot{v} + c_{vv}\dot{v}^2 + g} \quad (17)$$

$$y_{zmp} = b - \frac{(c - z_{zmp})(b_u\ddot{u} + b_v\ddot{v} + b_{uu}\dot{u}^2 + 2b_{uv}\dot{u}\dot{v} + b_{vv}\dot{v}^2)}{c_u\ddot{u} + c_v\ddot{v} + c_{uu}\dot{u}^2 + 2c_{uv}\dot{u}\dot{v} + c_{vv}\dot{v}^2 + g} \quad (18)$$

Where, $(\bullet)_u = \frac{\partial(\bullet)}{\partial u}$, $(\bullet)_v = \frac{\partial(\bullet)}{\partial v}$, $(\bullet)_{uu} = \frac{\partial^2(\bullet)}{\partial u^2}$, $(\bullet)_{uv} = \frac{\partial^2(\bullet)}{\partial u \partial v}$, $(\bullet)_{vv} = \frac{\partial^2(\bullet)}{\partial v^2}$. Two ZMP equations can be represented by two parametric variables. Since the COG motion is kinematically related with two parametric variables, a time response of the COG motion can be generated by the ZMP position by preparing constraint surface of the COG motion in world coordinates in advance.

B. Acquire the human's ZMP trajectory based on the human's COG image analysis

The marker is attached to acquire the human's COG trajectory in the sagittal plane and frontal plane as shown Fig. 3 and Fig. 6. The distortion caused by human's gait is bigger in size than marker and step length error. So camera executes the calibration and we acquire the result shown in Fig. 8(a). We can acquire the human's ZMP trajectory of human's COG trajectory show in Fig. 8(a) substitutions to Eq. (14) and Eq. (15).

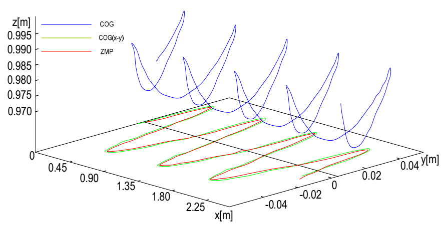

(a) COG and ZMP trajectory

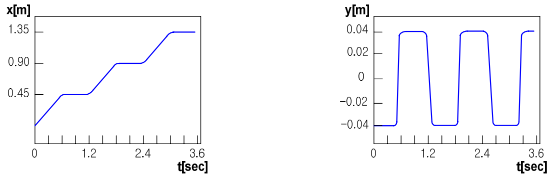

(b) ZMP trajectory in the sagittal plane (c) ZMP trajectory in the lateral plane

Fig. 8 Human's COG and ZMP trajectory

Fig. 8(a) shows the COG trajectory for gait. Fig. 8(b) shows the variation of the ZMP in x axis during the course of time. That is to say, ZMP increase linearly in the SSP, but that is not change temporary in the DSP. Fig. 8(c) is shown the variation of the ZMP in y axis during the course of time. And shows the certain pattern such as a sine wave form in the DSP.

IV. Human's Gait Pattern Analysis

Human's gait pattern image analysis, the angles, velocities, and accelerations of the joints of the human are shown in Fig. 9.

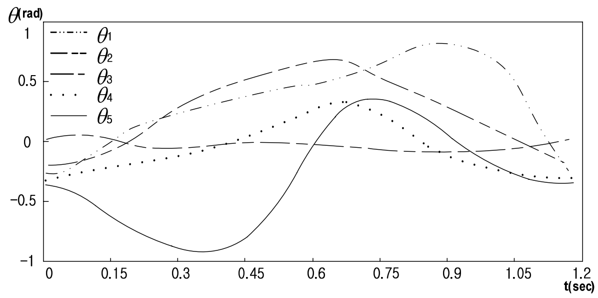

(a) Angles of human's joint

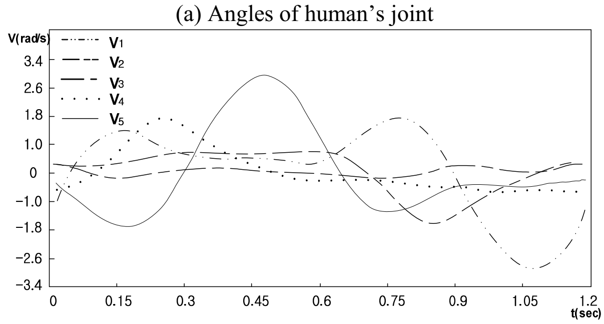

(b) Velocities of angles of human's joint

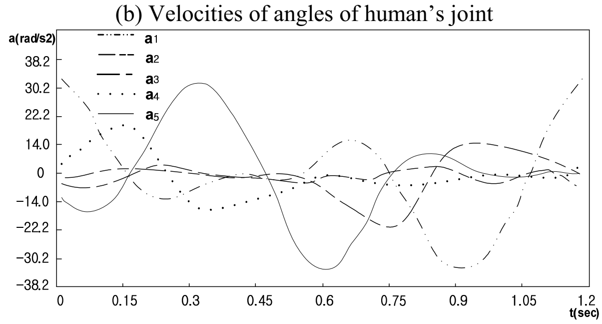

(c) Accelerations of angles of human's joint

Fig. 9 Rotation components of Human's joints during one period gait

Fig. 9(a) is shows joint's the angles by using the joint's pose acquired gait image. The joint's velocities of angles is calculated by differentiating with joint's angles, as shown in Fig. 9(b). The joint's accelerations of angles is derived from calculating the joint's velocities of angles, as shown Fig. 9(c).

The human's values are given as Table.1 This is average human values. And human's torques are obtained by Lagrangian equation Eq. (6) as shown in Fig. 10.

TABLE I
Human's Gait Values

Link	$M_i(kg)$	$l_i(m)$	$d_i(m)$	$I_i(kg{\bullet}m^2)$
1	3.355	0.48735	0.192	0.137
2	5.500	0.41895	0.237	0.101
3	37.290	0.80370	0.503	5.925
4	5.500	0.41895	0.181	0.101
5	3.355	0.48735	0.295	0.137

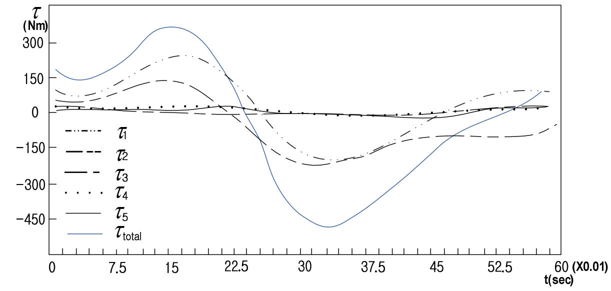

Fig. 10 Human's calculated torques

V. Generation of the 5-Link Biped Robot's Gait Pattern

The gait is constructed by motions at 3D plane makes up the sagittal, frontal, transverse plane. As shown in Fig. 1, the sagittal plane is the human's side as X-Z plane, the frontal plane is the human's side as Y-Z plane, the transverse plane is the human's side as X-Y plane. This planes cross at right angles mutually. So if we know motions in two planes, we can restore 3D motions. This paper generates the natural and stable 5-link biped robot by generating the gait trajectory in the sagittal and frontal plane.

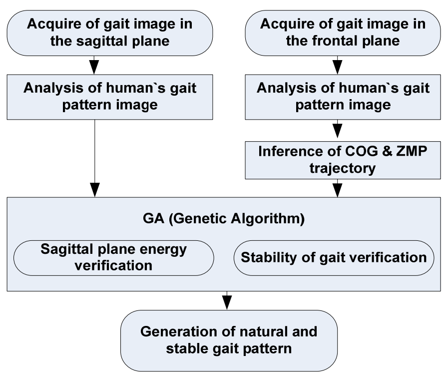

Fig. 11 Flow of the proposed algorithm

The proposed algorithm presented is shown in Fig. 11. Since a lot of the control parameters of robot's joints aren't acquired from ZMP and joint torques, the GA (Genetic Algorithm) is used to adaptively search the optimal solution of them.

A. Generation of the adaptive 5-link biped robot's gait pattern

The algorithm for the adaptive 5-link biped robot's gait pattern using the human's gait pattern is shown in Fig. 12.

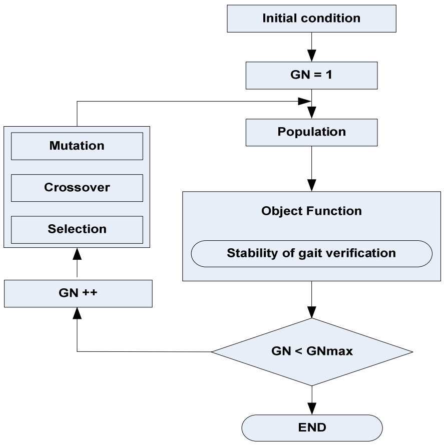

Fig. 12.Flow of the gait pattern generation using GA

This paper defines fitness function of the GA for sagittal plane gait as shown in Eq. (19).

$$f_1 = \int_0^{t_c} E_{FDC}\, dt \tag{19}$$

Where t_c is the gait cycle, E_{FDC} is the absolute error value between the human's gait torque and 5-link biped robot given in Eq. (20).

$$E_{FDC} = \| H_{FDC} - R_{FDC} \| \tag{20}$$

Where H_{FDC} expresses human's joint torque during one period of the gait, and R_{FDC} expresses the 5-link biped robot's joint torque during one period of gait.
The fitness function of the GA for the gait pattern on the frontal plane is defined as Eq. (21), Eq. (22).

$$f_2 = \int_0^{t_c} E_{ZMP}\, dt \tag{21}$$

$$E_{ZMP} = \| p_{dZMP} - p_{ZMP} \| \tag{22}$$

p_{ZMP} and p_{dZMP} are calculated ZMP trajectory and the human's ZMP trajectory, respectively.

VI. Experiments applied to 5-link biped robot model

The sequential images for image analysis are acquired through two CCD digital camera (IPX-VGA 210) in the sagittal and frontal plane. Human's gait pattern is composed of total 120 frames during a step. The experimentation is carried out described in this paper using human gait. The proposed algorithm's performance evaluates to use the 5-link biped robot simulator (5-LBRS) that is implemented using VC++ of Pentium PC.

Generally gait patterns are evaluated by natural, stable and lower energy gait pattern. The Human's values are given as Table. 2.

TABLE 2
HUMAN'S GAIT VALUES

Link	$M_i(kg)$	$l_i(m)$	$d_i(m)$	$I_i(kg\cdot m^2)$
1	5.159	0.47531	0.174	0.152
2	7.115	0.39341	0.209	0.121
3	38.452	0.80128	0.497	6.047
4	7.115	0.39341	0.169	0.152
5	5.159	0.47531	0.287	0.121

A. Extraction of human's gait values and measurement of the ZMP

We measure the human's COG variation for acquiring the human's gait values and ZMP trajectory. The angles of human's joints are shown Fig. 13. As shown Fig. 14, the torques of human's joints are acquired by substitution dynamics model Eq. (6), Eq. (9) for the angles of human's joints and link's values.

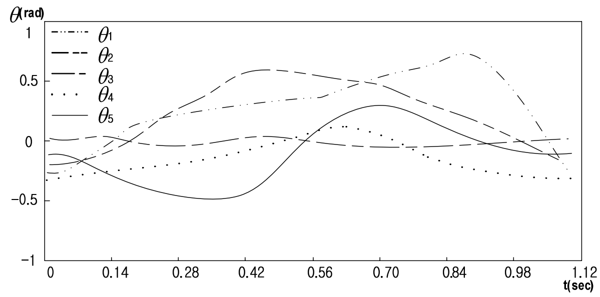

Fig. 13 Rotation angles of Human's joints during one period gait

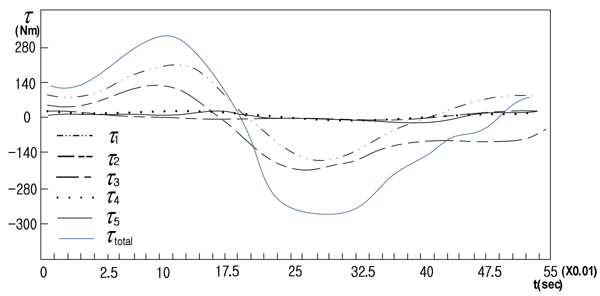

Fig. 14 Human's torques calculated from dynamics model

The human's COG and ZMP trajectory measured in the sagittal and frontal plane are shown Fig. 15.

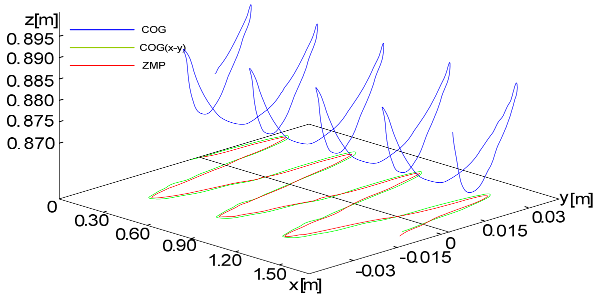

Fig. 15 Human's COG & ZMP trajectory measured from gait images

B. *Generation of the 5-link biped robot's gait pattern*

We generate the adaptive 5-link biped robot's pattern using the genetic algorithm. Initial populations are given from a cubic spline interpolation method. The specifications of the 5-link biped robot are given in Table 3, and the GA specifications are given in Table 4.

TABLE 3
SPECIFICATIONS OF 5-LINK BIPED ROBOT MODEL

LINK	$M_i(kg)$	$l_i(m)$	$d_i(m)$	$I_i(kg \bullet m^2)$
1	0.164	0.115	0.032	0.00082
2	0.144	0.085	0.053	0.00060
3	0.422	0.110	0.091	0.00350
4	0.144	0.085	0.032	0.00060
5	0.164	0.115	0.053	0.00082

TABLE 4
SPECIFICATIONS OF GA

Maximum Generation (GN_{max})	300
Population Size	50
Crossover Probability	0.98
Mutation Probability	0.05

The 5-link biped robot model's torque that is generated by adaptive algorithm of the gait pattern generation is shown Fig. 16. The 5-link biped robot's torque is convergence to the human's torque that is shown Fig. 14. The 5-link biped robot's torque is acquired by using the genetic algorithm, as shown Fig. 17.

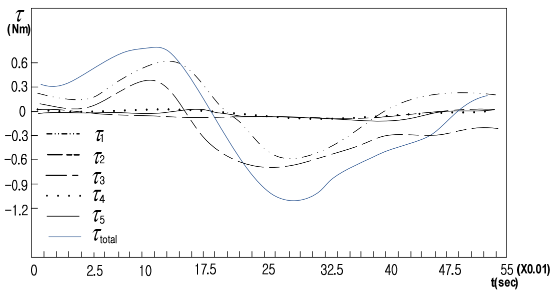

Fig. 16 Calculated robot's torques in proposed algorithm

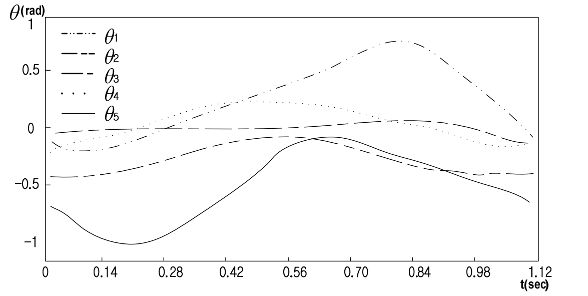

Fig. 17 Rotation angles of individual robot's joints acquired using the proposed algorithm

The human's COG and ZMP trajectory generated for stable of the 5-link biped robot's are shown Fig. 18.

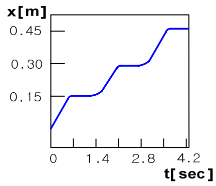

(a) ZMP trajectory in sagittal plane

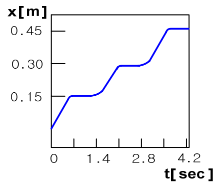

(b) ZMP trajectory in lateral plane

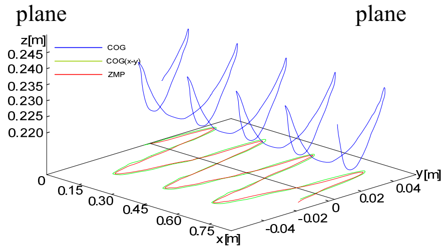

(c) COG and ZMP trajectory

Fig. 18 5-link biped robot's COG and ZMP trajectory

Fig. 18(a) shows the variation of the ZMP in the side of x-axis during the course of time. Fig. 18(b) is shown the variation of the ZMP in the side of y-axis during the course of time. Fig. 18(c) is shown the stable gait pattern. Because the 5-link biped robot's ZMP is posed inner COG trajectory projected to the X-Y plane. The 5-link biped robot's COG and ZMP is alike to the human's gait pattern as shown Fig. 14.

The 5-link biped robot's pattern is shown Fig. 19 and Fig. 20.

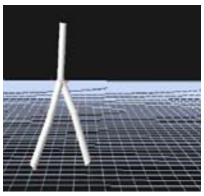
t = 0.0 (sec)

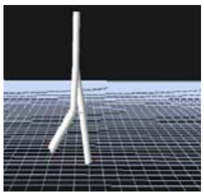
t = 0.28 (sec)

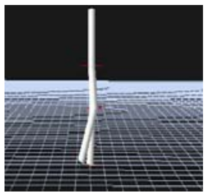
t = 0.56 (sec)

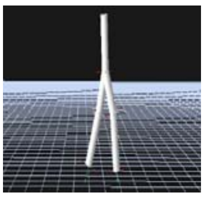
t = 0.84 (sec)

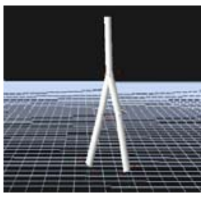
t = 1.12 (sec)

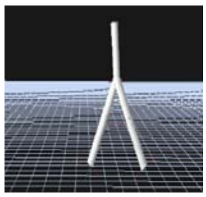
t = 1.4 (sec)

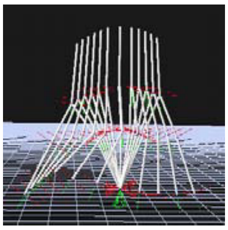

Fig. 19 Simulation of 5-link biped robot in the sagittal plane

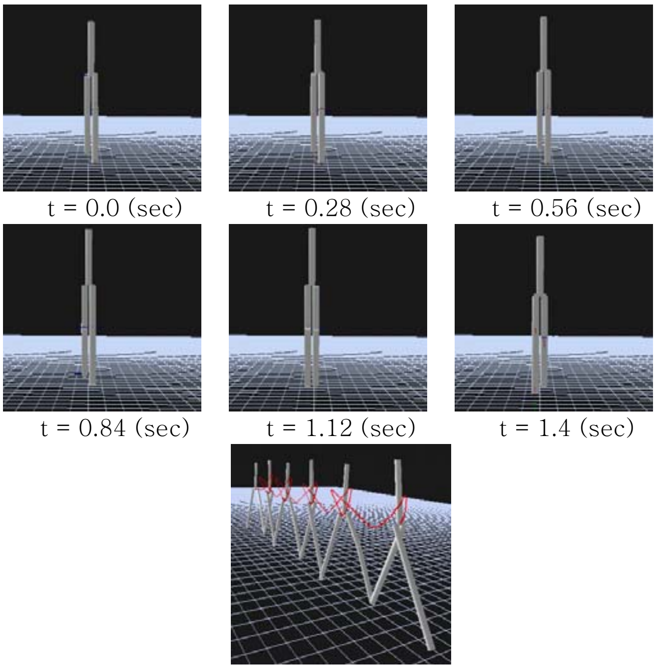

Fig. 20 Simulation of 5-link biped robot in the frontal plane

Because of gait pattern generation of the 5-link biped robot based on the human's gait pattern images, as shown Fig. 21, we can verify the stable gait pattern generation.

This paper demonstrate that the proposed algorithm is superior by evaluating the 5-link biped robot that is applied to each gait patterns made both in the general way using inverse kinematics and in the special way as proposed regarding energy efficiency. Evaluation of energy efficiency is given in Table 5.

TABLE 5
THE EVALUATION OF ENERGY EFFICIENCY OF PROPOSED GAIT PATTERN OF THE 5-LINK BIPED ROBOT

Joints	Proposed algorithm	Inverse kinematics
1	0.015550J	0.018682J
2	0.009256J	0.011756J
3	0.002178J	0.005804J
4	0.001346J	0.003730J
5	0.000942J	0.001754J
Total	0.019232J	0.022148J

The energy of the proposed gait pattern of the 5-link biped robot compared with that is acquired by inverse kinematics, the proposed algorithm is better about 0.002916J than existing algorithms.

VII. CONCLUSION

This paper proposes that natural gait of the 5-link biped robot such as human being by analyzing the COG trajectory of human's gait in the sagittal and frontal plane. The natural, stable and energy efficient 5-link biped robot pattern is generated based on the algorithm of the adaptive gait pattern generation. The energy of the proposed gait pattern of the 5-link biped robot, compared with that, is acquired by inverse kinematics. The gait pattern is generated by the proposed algorithm applied to 5-link biped robot. It is found to be a natural and good energy saver.

REFERENCES

[1] L. Magdalena, "Learning Gait Patterns for the Fuzzy Synthesis of Biped Walk," *IEEE IFCIS*, pp.248-250, 1994.
[2] Q. Huang, "Planning Walking Patterns for a Biped Robot," *IEEE ICRA* Vol. 17, pp. 280-289, 2001.
[3] L. Endo, "Co-evolution of Morphology and Walking Pattern of Biped Humanoid Robot using Evolutionary Computation-Evolutionary Designing Method and its Evaluation," *IEEE IROS*, Vol. 1, pp. 340-345, 2003.
[4] M. Vukobratobic and D. Juricic, "Contribution to the Synthesis of Biped Gait," *IEEE Trans. Bio-Med. Eng*, Vol. 1, pp. 1-6, 1996.
[5] S. Kajita, F. Kanehiro, K. Kaneko, k. Yokoi and H. Hirukawa, "The 3D Linear Inverted Pendulum Mode : A simple modeling for a biped walking pattern generation," *Proc. of the 2001 IEEE/RSJ*, Vol. 1, pp. 239-246, 2001.
[6] Q. Huang, K. Shuuji, N. Koyachi, K. Kaneko, K. Yokoi, H. Arai, K. Komoriya and K. Tanie, "A High Stability, Smooth Walking pattern for a Biped Robot," *IEEE ICRA*, pp. 65-71, 1999.
[7] Arbulu, "ZMP Human Measure System," *IEEE Climbing-Walking Robots*, pp. 433-440, 2006.
[8] M. Morisawa, S. kajita, K. Kaneko and K. Harada, "Pattern Generation of Biped Walking Constrained on Parametric Surface," *IEEE ICRA*, pp. 2405-2410, 2005.
[9] Y. Hasegawa, "Trajectory Generation for Biped Locomotion Robot," *Mechatronics*, Vol. 10, pp. 67-89, 2000.
[10] A. Borghese, L. Bianchi and F. Lacquaniti, "Kinematic determinants of Human Locomotion," *Journal of Physiology*, pp. 863-879, 1996.
[11] Xiuping Mu and Qiong Wu, "A Complete dynamics model of five-link bipedal walking," *Proceeding of american control Conference*, pp. 4926-4931, 2003.
[12] Xiuping Mu and Qiong Wu, "Development of a complete dynamic model of a planar five-link biped and sliding mode control of its locomotion during the double support phase," *Int. Journal of control*, Vol. 77, no. 8, pp. 789-799, 2004.
[13] S. Kajita and K. Tani, "Study of Dynamic Biped Locomotion on Rugged Terrain," *ICAR*, Vol. 1, pp.741-746, 1991.